JOM, Vol. 73, No. 1, 2021
https://doi.org/10.1007/s11837-020-04474-0

A Review of Slag Refining of Silicon Alloys

SRIDEVI THOMAS ,[1,5] MANSOOR BARATI,[1] and KAZUKI MORITA[1,2]

1.—Department of Materials Science and Engineering, University of Toronto, 184 College St., Toronto, ON M5S 3E4, Canada. 2.—Institute of Industrial Science, The University of Tokyo, 4-6-1 Komaba, Meguro-ku, Tokyo 153-8505, Japan. 5.—e-mail: sridevi.thomas@mail.utoronto.ca

Slag refining of silicon has been modified in recent years by combining the process with solvent refining, in which an alloy of silicon is first treated by slag and then solidified under controlled conditions to yield high-purity silicon crystals. This paper discusses the effect of alloying elements on the efficiency of slag treatment. A set of criteria are established and quantified for potential alloying elements to guide their proper selection.

List of Symbols

(i)	Concentration of impurity i (B/P) in slag
$[i]$	Concentration of impurity i (B/P) in metal
$a_{O^{2-}}$	Activity of oxygen ions in slag
p_{O_2}	Oxygen potential
$\gamma_{impurityoxide}$	Activity coefficient of impurity oxide in slag
γ_i	Activity coefficient of impurity i in metal
a_{Si}	Activity of silicon

INTRODUCTION

Solar-grade silicon of 6–8 N purity is mainly produced by blending ultrapure, electronic-grade silicon (8–9 N), which is generated by the expensive and energy-intensive Siemen's method, with upgraded metallurgical grade silicon (3–5 N). Research in this field has been largely directed towards developing high-throughput methods that can achieve solar-grade purity in fewer steps or by a simpler process. The focus of purification is on removal of boron (B) and phosphorus (P), as these two elements are the most challenging to eliminate. To this end, significant effort has been expended to study slag and solvent refining, methods that are considered straightforward and thermodynamically feasible. A number of review papers on both methods have been published,[1–3] but recently a third approach has emerged: a combination of solvent and slag refining. The objective is to use a slag to treat an alloy of silicon at first to remove B and P, followed by controlled cooling of the alloy to achieve high-purity silicon phases, leaving the remainder of the B and P in the alloy phase.

A review article published along with this paper discusses slag refining of silicon metal with the following key takeaways:

1. The basicity ($a_{O^{2-}}$) and oxygen potential (p_{O_2}) of the slag work in tandem to maximize B and P removal from silicon.
2. To quantify the efficacy of slag refining, the distribution coefficient, L_i, was defined as the ratio of the concentration of the impurity in the slag to that in the silicon, $L_i = x_{i,slag}/x_{i,metal}$.
3. L_i is usually too low to allow effective removal of B/P to a desired concentration with a reasonable slag mass.
4. Alloying the silicon with another metal can lessen or enhance the removal of B and P by slag, as it affects the activity of the impurity in the alloy.

In directional solidification of silicon, Si crystals are grown out of a liquid pool, leaving the impurities in the liquid. The distribution of impurities between liquid and solid Si is quantified by the segregation coefficient k, expressed in Eq. 1, where a smaller k represents better removal.

(Received June 24, 2020; accepted October 27, 2020; published online November 19, 2020)

$$k = \frac{\text{Impurity in solid}}{\text{Impurity in liquid}} \quad (1)$$

In the modified process of directional solidification known as solvent refining, an alloying element, referred to as a "getter," is added to Si to improve the retention of the impurities in the liquid. It has been shown[4–8] that alloying elements such as Al, Fe, and Cu promote the retention of some impurity elements (P and B) in a liquid alloy, over that in an only liquid silicon metal. As the alloy cools, silicon dendrites form and precipitate out, while most impurities are rejected to the liquid alloy. Once an acceptable yield of silicon is precipitated out, the alloy is quenched, and the phases are separated by either physical (e.g., gravity separation) or chemical methods (e.g., leaching). It is also possible to remove the liquid alloy at a high temperature by filtration or decantation. A detailed review has been published[1] on the principles and effectiveness of a variety of metals that have been used as getters.

Different getter elements have been used with varying degrees of success, but no one getter element has been able to lower B and P concentrations to acceptable limits in one run when added in commercially acceptable quantities. As a next logical step, to benefit from the impurity removal of both solvent refining and slag treatment, the hybrid solvent refining-slag treatment method has been put forward. In this method, an alloy of Si-*X* (*X* being the getter element) is first treated with slag and then undergoes controlled solidification. Interesting observations have been made; for example, a few studies conducted on slag treatment of Si alloys have shown significantly higher L_B values than during slag refining of just silicon. This presents an opportunity to achieve dual and improved refining of Si by both mechanisms (slag treatment and solvent refining) at the same time, and possibly achieve SoG-Si purity levels in one process.

This article focuses on slag refining of silicon alloys and compares the works already conducted in this area. The paper further attempts to define what makes an effective alloying agent and lists properties that can aid future researchers in narrowing down the list of elements that are worth studying.

EFFECT OF ALLOYING ON IMPURITY BEHAVIOR

Slag treatment of silicon alloys removes boron and phosphorus as borates, phosphates, or phosphides. The corresponding reactions are shown in Eqs. 2, 3, and 4. The slag capacity, presented in Eqs. 5, 6, and 7, for borate, phosphate, and phosphide is useful when comparing the effect of the slag composition, provided that the metal is the same in each study, i.e., silicon. However, as soon as an alloy is employed, a different entity must be utilized as γ_i and a_{Si} can significantly affect the result. The normalized distributions shown in Eqs. 8, 9, and 10 illustrate that D_i is dependent on temperature (C_x), the composition of the metal/alloy (affecting γ_i and a_{Si}), and the composition of the slag (affecting p_{O_2}, $a_{O^{2-}}$, and $\gamma_{impurityoxide}$). If the activity of the impurity is high in the alloy, it is encouraged to move into the slag phase, even if the slag has no particular affinity for said impurity. To this end, the normalized distribution, D_i, can be used in conjunction with the optical basicity of slag to compare the effect of the alloy on the partition coefficient without the interference of oxygen potential (p_{O_2}). Optical basicity allows the comparison of different slags that may have similar end results due to their similar basicity. However, the γ_i values of B or P in many metals used in silicon alloys are not readily available; these gaps in fundamental knowledge need to be filled.

$$[B] + \frac{3}{2}O^{2-} + \frac{3}{4}O_2 \leftrightarrow \left(BO_3^{3-}\right) \quad (2)$$

$$[P] + \frac{3}{2}O^{2-} + \frac{5}{4}O_2 \leftrightarrow \left(PO_4^{3-}\right)(\text{high } p_{O_2}) \quad (3)$$

$$[P] + \frac{3}{2}O^{2-} \leftrightarrow \left(P^{3-}\right) + \frac{3}{4}O_2(\text{low } p_{O_2}) \quad (4)$$

$$C_{BO_3^{3-}} = \frac{(B)}{[B]} \cdot \frac{1}{(p_{O_2})^{3/4}} \cdot \frac{1}{\gamma_B} = C_2 \cdot \frac{\left(a_{O^{2-}}\right)^{\frac{3}{2}}}{\gamma_{BO_3^{3-}}} \quad (5)$$

$$C_{PO_4^{3-}} = \frac{(P)}{[P]} \cdot \frac{1}{(p_{O_2})^{5/4}} \cdot \frac{1}{\gamma_P} = C_3 \cdot \frac{\left(a_{O^{2-}}\right)^{\frac{3}{2}}}{\gamma_{PO_4^{3-}}} \quad (6)$$

$$C_{P^{3-}} = \frac{(P)}{[P]} \cdot \frac{(p_{O_2})^{3/4}}{1} \cdot \frac{1}{\gamma_P} = C_4 \cdot \frac{\left(a_{O^{2-}}\right)^{\frac{3}{2}}}{\gamma_{P^{3-}}} \quad (7)$$

$$D_{B,\text{borate}} = \frac{(B)}{[B]} \cdot \frac{1}{(p_{O_2})^{3/4}} = C_2 \cdot \frac{\left(a_{O^{2-}}\right)^{\frac{3}{2}}(\gamma_B)}{\gamma_{BO_3^{3-}}} \quad (8)$$

$$D_{P,\text{phosphate}} = \frac{(P)}{[P]} \cdot \frac{1}{(p_{O_2})^{5/4}} = C_3 \cdot \frac{\left(a_{O^{2-}}\right)^{\frac{3}{2}}(\gamma_P)}{\gamma_{PO_4^{3-}}} \quad (9)$$

$$D_{P,\text{phosphide}} = \frac{(P)}{[P]} \cdot \frac{(p_{O_2})^{3/4}}{1} = C_4 \cdot \frac{\left(a_{O^{2-}}\right)^{\frac{3}{2}}(\gamma_P)}{\gamma_{P^{3-}}} \quad (10)$$

Most studies in this area focus on the slag and alloy composition, and choosing an operating temperature that allows both slag and metal phases to be liquid. However, temperature affects the equilibrium constant of the reactions between slag and metal, and there is a clear distinction between

studies conducted at different temperatures; the higher the temperature the more detrimental to L_B (not enough data for L_P).

Data from nine papers were used to compare the normalized distribution of the slag systems. These papers were chosen because the authors reported the initial and final composition of the slag and other experimental details that were necessary to calculate the activity of silicon and silicon dioxide using thermodynamic models. In some instances, the composition of the slag changes throughout the experiment, which could lead to the reversion or reaction of B or P into the metal phase. However, the change in slag composition and the reversion of impurities can happen at different rates, so initial compositions of slag were used to plot D_i values against optical basicity. Unless mentioned in the study, phosphorus was assumed to be removed as phosphate.

It is imperative to note that the slag systems differ from study to study, and although optical basicity is employed to make as fair a comparison, in some systems, the presence of certain oxides improves the removal percentage of boron or phosphorus. For instance, the slag capacity for borate and phosphate is considerably improved when sodium oxide is added. To this end, a list of slag systems and the corresponding metals is presented in Table I.

Figure I compares the D_B values of the silicon metal and alloy systems. When comparing the data for silicon–slag systems, it is clear that, at 1500°C, the system achieves higher D_B than at 1600°C. This phenomenon can be explained by the exothermic nature of the oxidation of boron into the slag, which is hindered at higher temperatures.

Plotted alongside Jakobsson's data[10] are data available from White et al.[11] White worked with an Ar + CO atmosphere in the presence of a graphite crucible to create an equilibrium between CO and C and establish a known oxygen potential, p_{O_2}, in the atmosphere. However, as can be seen from Fig. 1, the data are very similar to the experiments conducted in a pure argon atmosphere. It may be possible that either Jakobsson did not scrub their argon of the trace oxygen, establishing a p_{O_2} close to that of White, or the reaction in White's system was not in full gas–metal–slag equilibrium. It is also worthwhile to note that both Jakobsson and White used MgO in their slag systems, and it appears that MgO can replace CaO as long as the final basicity remains unaffected.

Comparing the alloy systems at 1500°C, it appears that using a copper-silicon system is conducive to removing boron. The activity coefficients listed in Table II show that γ_B in copper is higher than in silicon, leading to a higher B activity in a copper-silicon alloy. This in turn should lead to a higher partition coefficient than if a simple silicon–slag system were utilized, and at first glance, this is indeed the case for the same basicity of slag used. However, it should be noted that Li's slag[8] contained sodium oxide, and ideally, the same slag system for both silicon and silicon alloy should be used to enable a fair comparison on the effect of alloying. Huang's copper-silicon system[13] at 50°C higher did not use sodium oxide, and they reported lower L_B values, but it is not clear whether this is a result of the lack of Na_2O or the higher operating temperature. Furthermore, the D_B value for Huang's system is closer to the silicon system at 1600°C, and Cu appears not to have improved the B rejection into the slag. Huang worked with a lower copper content in their alloy, and this most likely lowered the activity of boron in the alloy, negatively impacting boron removal.

Although the tin-silicon alloy purification was conducted at a lower operating temperature of 1400°C, the copper-silicon D_B values (at 1500°C) are close, again possibly emphasizing the efficacy of sodium oxide. In this case, a quantitative comparison between Cu and Sn cannot be made as Cu-Si was 15–85 mol.% (30–70 wt.%) and Sn-Si was 30–70 mol.% (65–35 wt.%). Nonetheless, the authors[12] pointed out that the presence of tin increased the activity coefficient of B in the alloy, as they obtained higher L_B values with increased tin content. Al-Khazraji[14] also worked with a Sn-Si system at 75 wt.% Si and 1500°C, and the effect is twofold: the lower Sn concentration and higher operating temperature resulted in lower D_B values. The influence of each alloying element on B rejection may be evaluated by comparing D_B values at a given basicity, operating temperature, and percentage of alloying element.

Alloy slag refining conducted at 1600°C used very similar slag systems to silicon (CaO-MgO-Al_2O_3-SiO_2), which allows for a better comparison. The data show that iron does not affect the activity of B in the alloy system to the same extent as copper or tin. In fact, based on literature listed in Table II, iron lowers the activity of B in Fe-Si and can have a negative effect on B removal through slag refining; and the slightly higher D_B values compared with the pure Si data might be explained by the slag capacity, as shown in Fig. 3.

Figure 2 compares the D_P values of three systems: Si, Cu-Si, and Fe-Si. Unlike for B, Cu decreases the activity coefficient of P and hinders the rejection of P into the slag, which leads to comparable D_P values to pure Si, even in the presence of sodium oxide. In fact, one composition did not have any sodium oxide content (labeled on graph) and resulted in a much lower D_P value. Huang[13] also reported P removal using their Cu-Si system and reported lower L_P values, which can be credited to the higher working temperature and a sodium-oxide-free slag.

Fe-Si did not perform any better, although this can be attributed to the higher operating temperature. As Fig. 4 shows, the phosphate capacity for this system is comparable to that of Johnston's, and Table II indicates that Fe increases the activity of phosphorus in the alloy, thus theoretically

Table I. A list of the works studied in this paper

Author	Slag	Metal	Temperature (°C)
Johnston[9]	$BaO/MgO\text{-}CaO\text{-}SiO_2\text{-}Al_2O_3$	Si	1500
Jakobsson[10]	$CaO\text{-}MgO\text{-}SiO_2\text{-}Al_2O_3$	Si	1600
White[11]	$CaO\text{-}MgO\text{-}SiO_2$	Si	1600
Ma[12]	$CaO\text{-}SiO_2\text{-}CaF_2$	Sn-35 wt.%Si	1400
Li [8]	$Na_2O\text{-}CaO\text{-}SiO_2\text{-}Al_2O_3$	Cu-30 wt.%Si	1500
Huang[13]	$CaO\text{-}SiO_2\text{-}CaCl_2$	Cu-50 wt.%Si	1550
Al-Khazraji[14]	$CaO\text{-}SiO_2\text{-}CaCl_2$	Sn-75 wt.%Si	1500
Hosseinpour[15,16]	$CaO\text{-}SiO_2\text{-}Al_2O_3$	Fe-80 wt.%Si	1600

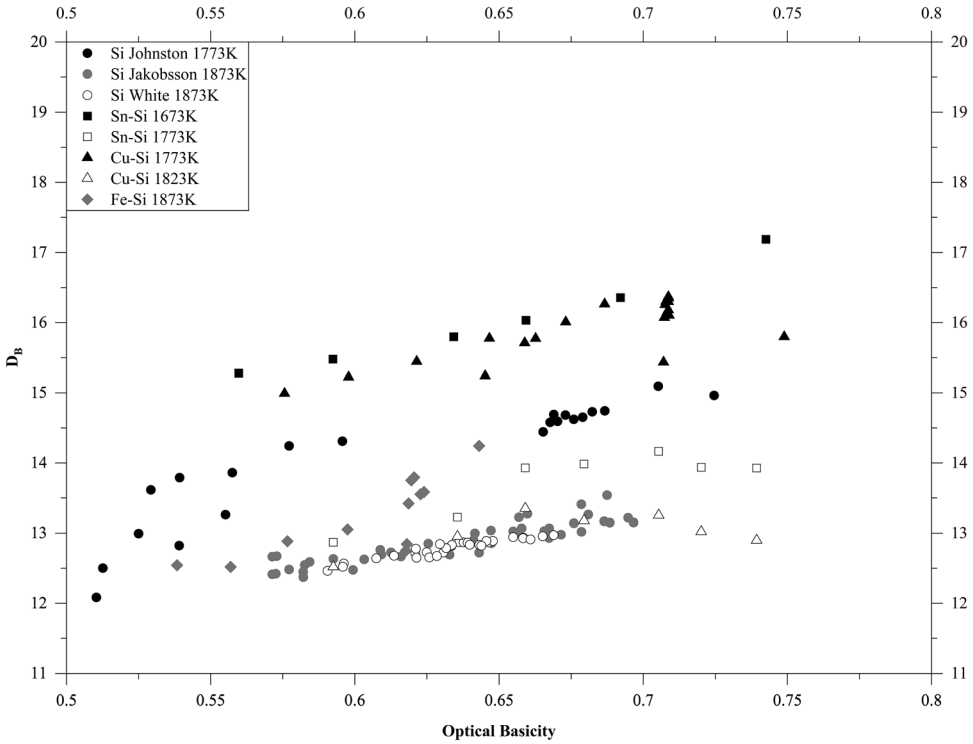

Fig. 1. Comparing the D_B values calculated from the works of Sn-Si, Cu-Si, and Fe-Si with Si.

Table II. A list of alloying metals and activity coefficients of boron and phosphorus

Metal (Temp. °C)	γ_B	γ_P
Silicon (1420, 1500, 1600)	3.91, 3.87, 3.84[17]	0.34, 0.37, 0.39[4]
Copper (1500)	$1.44<\gamma_B<10$ [18]	0.007[19]
Iron (1600)	0.026[20]	1.25[21]
Aluminum (1600)	3.30[22]	2.20[23]
Tin (1400)	65,000[24]	2.01[25]

The activity coefficients listed are for the temperatures indicated next to the metal

improving the P removal through slag refining. Phosphate capacities for a simple Si-slag system at 1600°C are not available to allow a proper comparison.

Slag capacities for both BO_3^{3-} and PO_4^{3-} were plotted to demonstrate that slag capacity cannot solely represent the effectiveness of slag refining of Si alloys. In Fig. 3, at 1500°C, Li's slag shows much

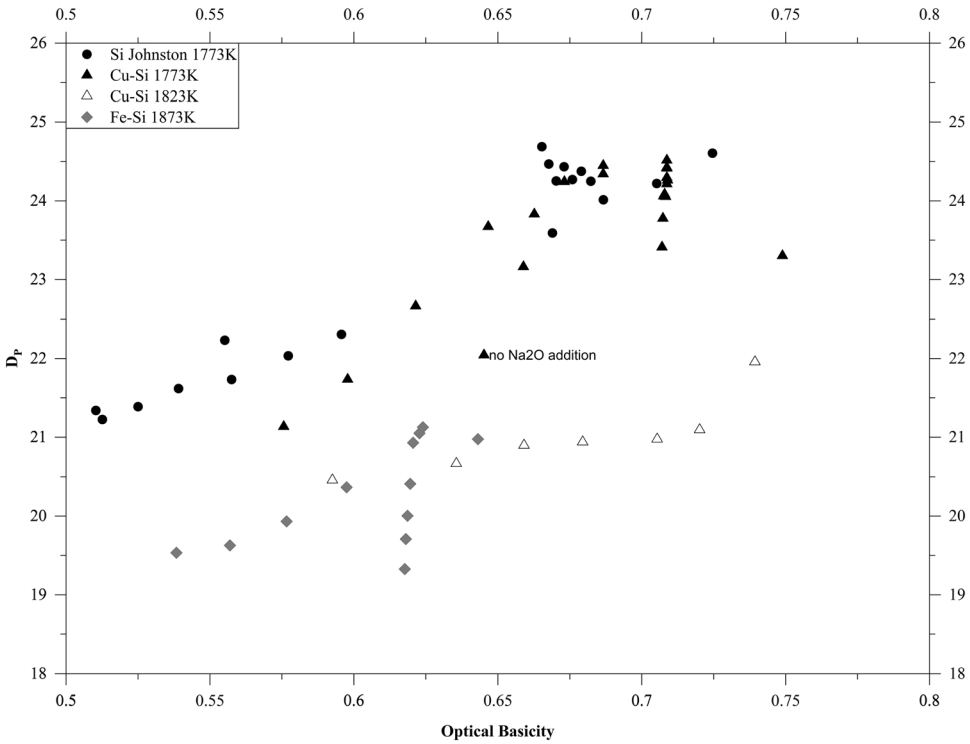

Fig. 2. Comparing D_P values calculated from the works of Cu-Si and Fe-Si with Si.

higher capacity for borate ions than Johnston's slag, most likely due to the presence of sodium oxide. The normalized distribution in Fig. 1 also shows higher values. On the other hand, for phosphorus removal, Fig. 4 shows that Li's slag has a higher capacity for phosphate ions compared with Johnston's, but the normalized distributions in Fig. 2 show similar values. This is where the role of the copper is emphasized; copper reduces the activity of P and depresses the partition coefficient. Similarly at 1600°C, in Fig. 3, Hosseinpour's slag has a much higher borate capacity compared with Jakobsson's slag, but the normalized distribution in Fig. 1 shows values closer to Jakobsson's, once again indicating that the presence of Fe decreases the activity of B and depresses the partition coefficient.

It is not completely fair to compare an alloy system with a pure silicon system when both studies employ different slags, since both the slag and the alloy composition heavily influence L_i values, which in turn impacts D_i and the slag capacity. However, it is also very clear that alloys can either improve or hinder the removal of B and/or P during slag refining, and future research should take this into consideration.

CRITERIA FOR EFFECTIVENESS OF ALLOYING ELEMENTS

The analysis above endeavored to demonstrate that the composition of the alloy can have a significant effect on the B and P removal by influencing the activity coefficients of these impurities in the alloy. The slag system should have a high capacity for borates and phosphates, but if the alloy has a high affinity for the impurities, then they are hindered from moving into the slag. To this end, it is beneficial to examine which alloy systems offer greater potential for purification of Si when a combination of slag and solvent refining is employed. In this section, various criteria for the alloying elements are considered, and the available data are compiled to provide a screening tool. Table III provides the pertaining information.

Suitability for Solvent Refining

The primary role of the alloying element (X) is to alloy with silicon and allow precipitation of purer Si from the melt by retaining impurities. This requires, firstly, that the alloying element itself does not remain in the silicon as an impurity (i.e., has a low solid solubility at the phase separation temperature) or can be easily removed from the semi-refined silicon (e.g., by subsequent melting and oxidation). Secondly, the segregation coefficient of the impurities in the Si-X alloy should be significantly less than in Si, to allow the retention of the impurities in the liquid alloy when Si crystals are precipitating. In thermodynamic terms, this implies that the activity coefficient of impurity in the Si-X alloy should be smaller than that in Si.

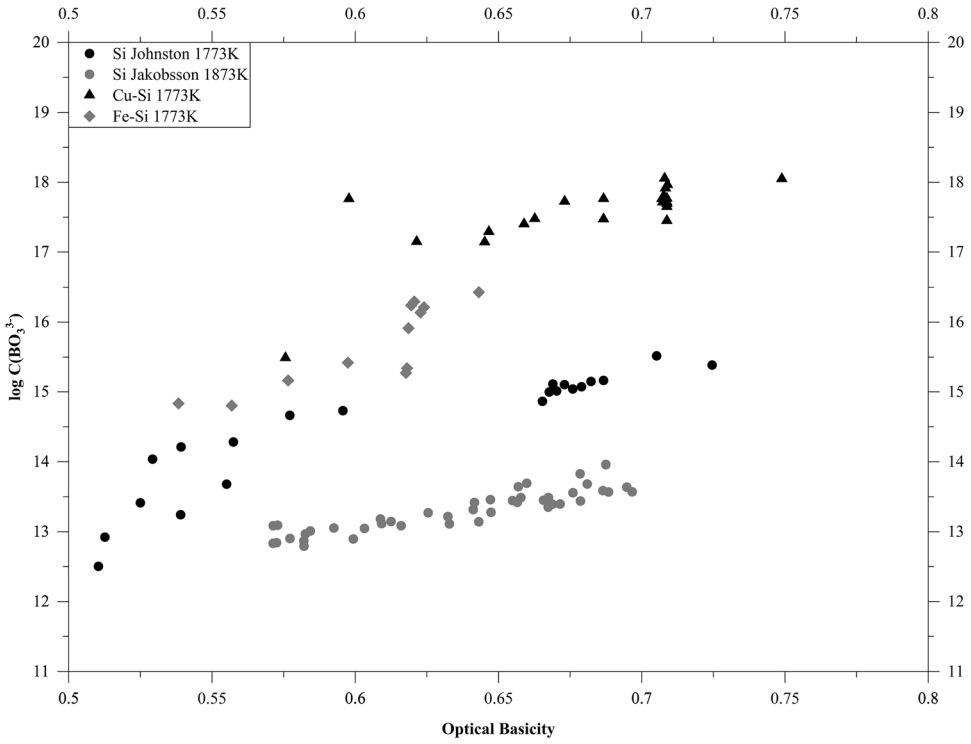

Fig. 3. Borate slag capacities for four different systems.

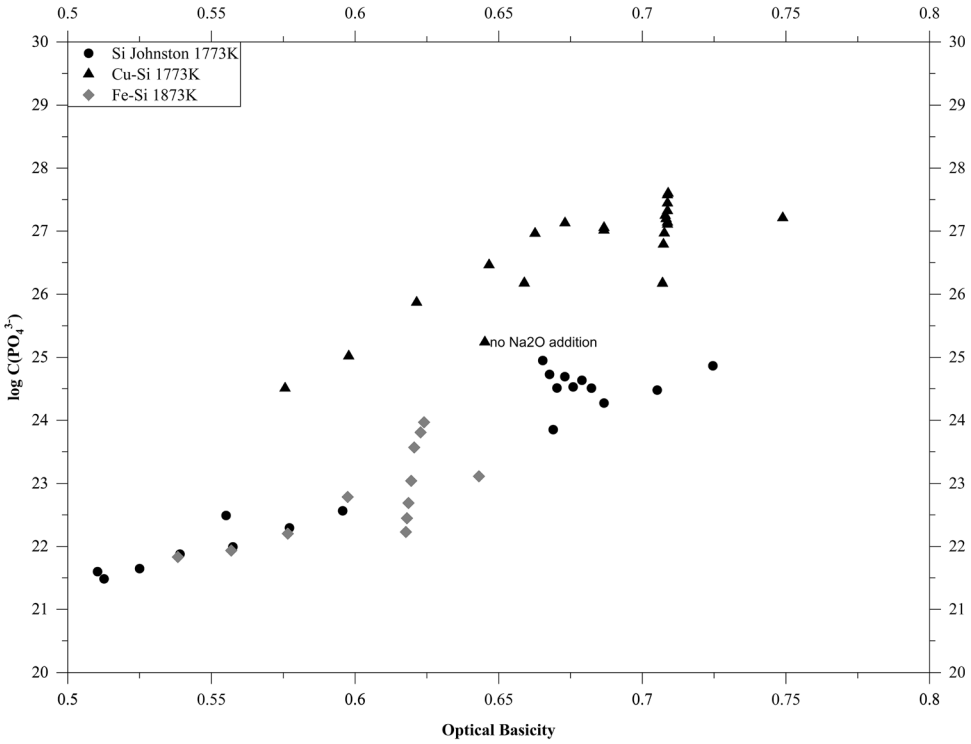

Fig. 4. Phosphate slag capacities for three different systems.

Promoting Slag Refining

The equilibrium between slag and alloy establishes an equal activity of an impurity in the two phases, as shown in Eq. 11. It is clear that, for a high distribution coefficient L_i, the impurity should have a high activity coefficient in the alloy and a low activity coefficient in the slag. Evidently, this contradicts the requirement stated above for solvent

Table III. Properties of interest for the selection of getter elements in a hybrid process

Alloying element (*X*)	Maximum solubility in solid Si (ppma)	Solubility in solid Si (ppma) at < 800°C*, 1000°C[§], or 1150°C[†]	Intermetallic with Si	Min. Si concentration in *X*-Si (wt.%)	C_B^* in *X* at 1400°C (wt.%)	*X*-B compound	C_P^* in *X* at 1400°C (wt.%)	*X*-P compound	Yield 1 (%)	Yield 2 (%)	Vapor pressure at 1500°C (Pa)
Silicon					1.5 (s)	SiB_6	1.9 (s)	SiP			16[j]
Boron	1.60%[a]	0.3 at.%*									
Phosphorus	2.60%[b]	2 at.%*									
Aluminum	428[c]	80*	None, eutectic	12.7	5.4 (l)	AlB_2	1.8 (l)	AlP	98.4	99.8	59 [k]
Antimony	1300[d]	300[§]	None	n/a	4.7 (l)	n/a	All liquid	n/a	100	100	~ 50,000 [l]
Barium	0[e]	0	$BaSi_2$	38.2	0.2 (l)	BaB_6	All liquid	n/a	93.1	95.5	~ 50,000 [l]
Bismuth	22[d]	1[†]	none	n/a	2.8 (l)	n/a	All liquid	n/a	100	100	~ 50,000 [l]
Calcium	2100[f]	500[†]	$CaSi_2$	64.5	0.9 (l)	CaB_6	63 ppm (l)	Ca_3P_2	79.8	84.4	~ 101,325 [l]
Chromium	0.097[d]	30 ppta[§]	$CrSi_2$	76.2	0 (s)	Cr_2B	5400 ppm (s)	Cr_3P	64.4	88.0	126[j]
Cobalt	1.1[d]	20 ppta*	$CoSi_2$	62.6	0 (s)	Co_3B	800 ppm (l)	Co_2P	81.4	89.4	0.8 [k]
Copper	34[g]	0.1*	$Cu_{19}Si_6$	17.0	All liquid	n/a	All liquid	Cu_3P	97.7	98.4	40 [k]
Gallium	610[d]	50*	None	n/a	0.2 (l)	n/a	13.0 (l)	GaP	100	100	~ 1000 [l]
Germanium	0 [h]	0	None	n/a	0.1 (l)	n/a	All liquid	GeP	100	100	33[j]
Indium	45[d]	0.1[§]	None	n/a	5.0 (l)	n/a	All liquid	InP	100	100	~ 2000 [k]
Iron	0.5[d]	100 ppta[§]	Fe_3Si_7	56.2	0 (s)	Fe_2B	2.0 (s)	Fe_3P	85.7	87.0	2 [k]
Lead	0 [h]	0	None	n/a	2.8 (l)	n/a	All liquid	n/a	100	100	~ 20,000 [l]
Magnesium	4100[f]	2000[†]	Mg_2Si	57.1	2.2 (l)	MgB_2	0.02 (l)	Mg_3P_2	85.2	93.6	> 101,325 [l]
Manganese	0.72[d]	1 ppba[§]	$Mn_{11}Si_{19}$	51.7	0 (s)	Mn_2B	All liquid	Mn_3P	88.1	90.2	~ 200 [l]
Nickel	23[d]	30 ppba*	$NiSi_2$	48.9	0 (s)	Ni_3B	0.07 (s)	Ni_3P	89.4	89.4	0.9 [k]
Tin	1600[d]	300*	None	n/a	0.002 (l)	n/a	All liquid	n/a	100	100	42 [k]
Titanium	0.025[d]	1 ppta*	$TiSi_2$	66.1	0 (s)	TiB	0.5 (s)	Ti_3P	78.3	87.0	0.03 [k]
Tungsten	2000[i]	< 2000[§]	Si_2W	78.0	0 (s)	W_2B	0.9 (s)	n/a	60.5	96.6	<< 1 [l]
Vanadium	0 [h]	0	Si_2V	94.6	0 (s)	V_3B_2	1.0 (s)	n/a	82.3	98.9	<< 1 [k]
Zinc	1.6[d]	5 ppba[§]	None	n/a	9.4 (l)	n/a	All liquid	Zn_3P_2	100	100	> 101,325 [l]
Zirconium	0 [h]	0	$ZrSi_2$	79.6	0 (s)	ZrB_2	0.6 (s)	n/a	56.8	93.2	<< 1 [k]

[a]Ref. 29.[b]Ref. 30.[c]Ref. 31.[d]Ref. 32.[e]Ref. 33.[f]Ref. 34.[g]Ref. 35.[h]Ref. 27.[i]Ref. 36.[j]Ref. 37.[k]Ref. 38.[l]Ref. 39.

refining; thus the significance of the activity coefficient of the impurity in the alloy (γ^i_{alloy}) needs to be looked at with care. For example, slag refining takes place at higher temperature than solvent refining, and the quantities are not simply comparable. Furthermore, the scale of refining is not linearly proportional to γ^i_{alloy} in the solvent refining and slag refining steps. In slag refining, the refining scales proportionally to the order of the reaction with respect to the impurity, whereas in solvent refining, the removal extent depends on the fraction of the alloy precipitating as purified Si. However, for the purpose of the hybrid process discussed here, the objective is the effectiveness of the slag treatment, as it serves as the primary means of refining the alloy (and hence refining of silicon). Also, a less effective slag refining process may be redundant to be included in the process in the first place. As a result, alloy systems with a greater γ^i_{alloy} are more favorable in the hybrid method.

$$x_{i,\text{slag}} \cdot \gamma_{i,\text{slag}} = x_{i,\text{alloy}} \cdot \gamma^i_{\text{alloy}} \tag{11}$$

Data on the activity coefficient of the element of interest in various Si-*X* alloy systems (γ^i_{alloy}) are scarce. As a result, ranking of alloys with regards to their effectiveness in rejection of impurities to slag is not directly possible for a wide range of alloy systems. However, the solubility limits of impurity *i* in metal *X* may be used as an indirect indication of the affinity between *i* and *X* (identified as C^*_i in Table III). The greater the solubility or the tendency to form compounds with B/P, the higher the affinity, i.e., the lower the activity coefficient. This approach ignores the ternary interactions of Si-*X*-*i* and, as a result, may be used as a preliminary screening tool for deciding whether a certain element *X* may be a viable candidate for the combined solvent refining–slag treatment approach.

Ease of Separation from Si

On completion of solvent refining, Si dendrites are separated from the remaining alloy by physical or chemical means. For example, in the case of Al, decantation of liquid alloy or segregation of dendrites using electromagnetic force[26] has been proposed. Alternatively, the residual Al-Si alloy can be leached using acid. The process implications, generation, and value of the byproducts of the process, and additional steps to further purify the remaining silicon, should be considered. Such considerations are not addressed in the present study as they lie beyond the fundamental perspective of this paper.

Minimizing Losses

The yield of Si when precipitated from the melt should be reasonably high, otherwise the materials handling and melting energy costs become prohibitively high. The yield can be calculated using

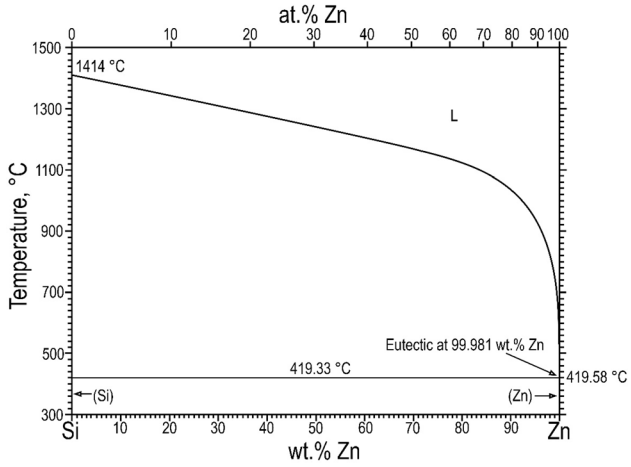

Fig. 5. Zn-Si phase diagram, reprinted with permission from Ref. 27.

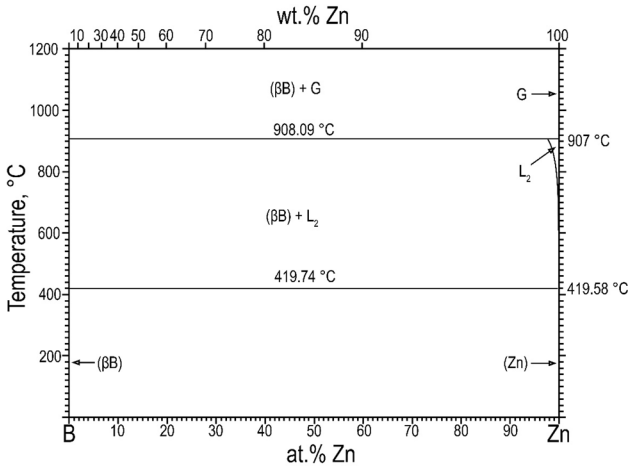

Fig. 6. Zn-B phase diagram, reprinted with permission from Ref. 28.

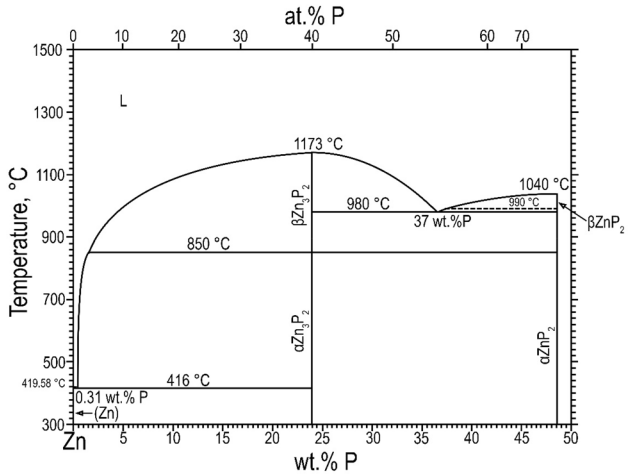

Fig. 7. Zn-P phase diagram, reprinted with permission from Ref. 27.

phase diagrams on the basis of the subsequent separation process. If the separation of Si from alloy is to be carried out at high temperature (e.g., liquid decantation or filtration of solids), the highest yield (identified as yield 1 in Table III) is the amount of Si

Table IV. A list of work done with slag refining of silicon alloys

Refs.	Slag composition	Alloy system	Temperature (K)	Slag-to-metal ratio	Atmosphere	Sample size (g)
Shin et al.[40]	$CaO-CaF_2$	Si-Mn	1823	2:1	CO diluted with argon	10.5
Ma et al.[12]	$CaO-SiO_2$-24 mol.%CaF_2	Si-Sn	1673	3:1	Argon	12
Li et al.[8]	$CaO-SiO_2-Na_2O-Al_2O_3$	Si-Cu	1773	10:1	Argon	11
Huang et al.[13]	$CaO-SiO_2-CaCl_2$	Si-Cu	1823	1:1	Ambient air	100
Li et al.[41]	5 wt.%CaO-25 wt.%SiO_2-70 wt.%Na_2SiO_3	Si-Sn	1723	1–2:1	Argon	20–30
Krystad et al.[42]	50 wt.%$CaO-SiO_2$	Si-Fe	1873	4:7	Argon	50
Al-khazraji et al.[14]	$CaO-SiO_2-CaCl_2$	Si-Sn	1773	1–2:1	Argon	?
Hosseinpour et al.[15]	$CaO-SiO_2-Al_2O_3$	Si-Fe	1873	1:1	Argon	10
Hosseinpour et al.[16]	$CaO-SiO_2-Al_2O_3$	Si-Fe	1873	1:1	Argon	10

Refs.	Equilibrium time (h) (confirmed, n/y)	Initial B/P content in slag/metal	Crucible	Stirring (y/n)	Final composition (y/n)	Highest L_i
Shin et al.[40]	12 (y)	?	Graphite	n	n	1.5 (P)
Ma et al.[12]	18 (y)	90–900 ppm B in alloy	Graphite	y (induction)	y	200 (B)
Li et al.[8]	10 min (y)	3000 ppm B + 3000 ppm P in alloy	Alumina	n	y	46.8 (B) 1.10 (P)
Huang et al.[13]	30 min	3 ppm B + 12 ppm P in alloy	Graphite	y (induction)	y	3 (B) 0.5 (P)
Li et al.[41]	3 (n)	13 ppm B in alloy	Graphite	n	n	7.7 (B)
Krystad et al.[42]	2	300 ppm B in alloy	Graphite	n	n	2.4 (B)
Al-khazraji et al.[14]	15 min (n)	14 ppm B in alloy	Graphite	n	n	5.7 (B)
Hosseinpour et al.[15]	8 (y)	?	Alumina	n	n	11.4 (B)
Hosseinpour et al.[16]	8 (y)	1000–1750 ppm P in alloy	Alumina	n	n	0.11 (P)

just above the critical temperature (e.g., eutectic). On the other hand, if the material is fully solidified, and chemical or physical means are employed for the recovery of Si, the yield (yield 2) is the amount of Si metal available at room temperature. In addition, the alloying element should not be reactive towards the slag itself (i.e., reduce the slag) or have a high vapor pressure at the refining temperatures.

As an example, the Zn-Si system is discussed in this section. Figure 5 shows the phase diagram for Zn-Si; at first glance, it is the ideal case where there is no intermetallic between the two elements, giving a high yield of Si, and Zn has a low solubility in Si. However, Zn has a high vapor pressure at high temperatures, therefore a low-melting-temperature slag has to be utilized for slag refining. Alternatively, the treatment can take place in a sealed and pressurized reactor, although this is practically challenging.

Figure 6 shows the Zn-B phase diagram, and it is clear that Zn has little to no solubility for B and does not form an intermetallic, which indicates a high activity coefficient for B, hence $\gamma_{B,Si-Zn}$ is expected to be larger than $\gamma_{B,Si}$. Figure 7 shows the Zn-P phase diagram, and Zn has a solubility for P and form intermetallics, which indicates that it may not be beneficial for forcing P to move into the slag. However, Zn-P is all liquid at 1400°C when Si solidifies; Zn can potentially retain P as pure Si starts precipitating out. Sometimes, however, it may be necessary to use two different alloying components to repel B and P individually.

This paper has compiled a list of viable alloying elements that may be worthy of further investigation in slag and solvent refining, listed in Table III. The table indicates whether the alloying element *X* forms an intermetallic with silicon, the maximum solubility of *X* in Si, whether it forms intermetallics with boron or phosphorus, the maximum solubility of B and P in the alloying element at 1400°C, and whether the element is in liquid (l) or solid (s) form. An ideal alloying element *X* should not form intermetallics with Si to increase the Si yield and should have low solubility in Si. Also, *X* should have low vapor pressure at the operating temperature and be easily separated from Si dendrites, either physically or chemically. The act of alloying should increase the activity of B and/or P in the system so as to encourage rejection into the slag by either not forming intermetallics with B or P, or having a very low solubility for B or P in the liquid state. Otherwise, *X* should have a much higher affinity for B or P, as indicated by high solubility limits for B and P in the solid state, such that, as silicon dendrites start precipitating, B and P are retained in the liquid phase by *X*. Finally, the yield of silicon dendrites should make the process economically viable. These criteria, when matched against those in Table III, should enable informed screening of suitable alloying candidates for an overall improvement of the solvent refining–slag treatment of silicon.

CONCLUSION

This paper looked at the effect of alloying on slag refining (Table IV) and found that removal percentages of B and P not only are functions of slag capacities but also depend on how the alloying element affects the activity of B and P. If the element increases the activity of the impurity, it encourages the removal of said impurity compared with just pure silicon using the same slag system; e.g., Sn encourages the removal of B. However, if the element decreases the activity of an impurity, it will adversely affect the removal of said impurity; e.g., Cu has such a high affinity for P that, even in a slag system that contained sodium oxide, it depressed the removal of P. In future studies, it would be useful to have data for both B and P removal, and use the same slag system to refine both Si and an alloy of silicon for a definitive comparative study. This paper also aimed to provide a list of viable alloying elements for future research in this field of study.

FUNDING

This study was funded by MITACS.

CONFLICT OF INTEREST

The authors declare that they have no conflicts of interest.

REFERENCES

1. M.D. Johnston, L. Tafaghodi-Kajavi, M.X. Li, S. Sokhanvaran, and M. Barati, *JOM* 64, 935 (2012).
2. R.K. Galgali, B.C. Mohanty, J.L. Gumaste, U. Syamaprasad, B.B. Nayak, S.K. Singh, and P.K. Jena, *Sol. Energy Mater.* 16, 297 (1987).
3. A.I. Journal, A. Hosseinpour, L.T. Khajavi, and A. Hosseinpour, *Miner. Process. Extr. Metall. Rev.* 39, 308 (2018).
4. T. Yoshikawa and K. Morita, *Sci. Technol. Adv. Mater.* 4, 531 (2004).
5. T. Yoshikawa and K. Morita, *Metall. Mater. Trans. B* 36, 731 (2005).
6. L.T. Khajavi and M. Barati, *High Temp. Mater. Process.* 31, 627 (2012).
7. L. Tafaghodi, K. Morita, T. Yoshikawa, and M. Barati, *J. Alloys Compd.* 619, 634 (2015).
8. M. Li, T. Utigard, and M. Barati, *Metall. Mater. Trans. B* 45, 221 (2014).
9. M.D. Johnston and M. Barati, *Sol. Energy Mater. Sol. Cells* 94, 2085 (2010).
10. L.K. Jakobsson and M. Tangstad, *Metall. Mater. Trans. B* 45, 1644 (2014).
11. J.F. White, C. Allertz, and S. Du, *Int. J. Mater. Res.* 104, 229 (2013).
12. X. Ma, T. Yoshikawa, and K. Morita, *Metall. Mater. Trans. B* 44, 528 (2013).
13. L. Huang, H. Lai, C. Gan, H. Xiong, P. Xing, and X. Luo, *Sep. Purif. Technol.* 170, 408 (2016).
14. R. Al-khazraji, Y. Li, and L. Zhang, *Metall. Res. Technol.* 115, 312 (2018).
15. A. Hosseinpour and L.T. Khajavi, *J. Alloys Compd.* 768, 545 (2018).

16. A.L.I. Hosseinpour and L.T. Khajavi, *Metall. Mater. Trans. B* 50, 1773 (2019).
17. T. Yoshikawa and K. Morita, *Mater. Trans.* 46, 1335 (2005).
18. K.T. Jacob, P. Shashank, and Y. Waseda, *Metall. Mater. Trans. A* 31, 2674 (2000).
19. M. Iwase, E. Ichise, and N. Yamada, *Steel Res.* 56, 319 (1985).
20. M. Yukinobu, O. Ogawa, and S. Goto, *Metall. Mater. Trans. B* 20, 705 (1989).
21. S. Ban-ya and M. Suzuki, *Iron Steel Inst. Jpn.* 61, 2933 (1975).
22. T. Yoshikawa and K. Morita, *J. Jpn. Inst. Met.* 68, 390 (2004).
23. B. Ban, X. Bai, J. Li, Y. Li, and J. Chen, *Metall. Mater. Trans. B* 46, 2430 (2015).
24. X. Ma, T. Yoshikawa, and K. Morita, *J. Alloys Compd.* 529, 12 (2012).
25. M.-C. Heuzey and A.D. Pelton, *Metall. Mater. Trans. B* 27B, 810 (1996).
26. T. Yoshikawa and K. Morita, *J. Cryst. Growth* 311, 776 (2009).
27. H. Baker, *ASM Handbook Alloy Phase Diagrams*, 10th ed. (Novelty: ASM, 1992).
28. H. Okamoto, *J. Phase Equilib. Diffus.* 36, 644 (2015).
29. A. Mostafa and M. Medraj, *Materials (Basel)* 10, 676 (2017).
30. F.A. Trumbore, *Bell Syst. Tech. J.* 39, 205 (1960).
31. T. Yoshikawa and K. Morita, *J. Electrochem. Soc.* 150, G465 (2003).
32. T. Yoshikawa, K. Morita, S. Kawanishi, and T. Tanaka, *J. Alloys Compd.* 490, 31 (2010).
33. M. Pani and A. Palenzona, *J. Alloys Compd.* 454, L1 (2008).
34. S. Kawanishi and T. Yoshikawa, *Mater. Trans.* 58, 450 (2017).
35. T. Yoshikawa and K. Morita, *J. Phys. Chem. Solids* 66, 261 (2005).
36. A. De Luca, A. Portavoce, and M. Texier, *J. Appl. Phys.* 115, 013501 (2014).
37. W.E. Forsythe, *Smithsonian Physical Tables*, 9th ed. (Washington: Smithsonian Institution Press, 1946).
38. D.R. Lide, *CRC Handbook of Chemistry and Physics*, 84th ed. (Boca Raton: CRC Press LLC, 2003).
39. G.W.C. Kaye and T.H. Laby, *Tables of Physical and Chemical Constants and Some Mathematical Functions*, 8th ed. (New Delhi: National Physical Laboratory, 1936).
40. J.H. Shin and J.H. Park, *Metall. Mater. Trans. B* 43, 1243 (2012).
41. J. Li, P. Cao, P. Ni, Y. Li, and Y. Tan, *Sep. Sci. Technol. Technol.* 51, 1598 (2016).
42. E. Krystad, L.K. Jakobsson, K.A.I. Tang, and G. Tranell, *Metall. Mater. Trans. B* 48, 2574 (2017).